Journal of Sound and Vibration (2001) **239**(2), 255–273
doi:10.1006/jsvi.2000.3115, available online at http://www.idealibrary.com on IDEAL®

SOUND PROPAGATION IN CIRCULAR DUCTS LINED WITH NOISE CONTROL FOAMS

Y. J. KANG AND I. H. JUNG†

School of Mechanical Engineering, Seoul National University, San 56-1 *Shinlim-Dong, Kwanak-Ku, Seoul* 151-742, *South Korea. E-mail yeonjune@snu.ac.kr*

(*Received* 20 *January* 1999, *and in final form* 26 *May* 2000)

Finite element predictions and corresponding measurements for sound attenuation and phase speed in a circular duct lined with poroelastic noise control foams are presented in this article. In the present study, four configurations having different lining thickness are considered for three types of foam samples. An axisymmetric foam finite element formulation based on Biot's theory is presented. The macroscopic physical properties of the foam lining samples were estimated using an optimization procedure based on measured physical and acoustical data. The results are also compared with Morse's local reaction solutions. The effects of lining thickness and foam properties on the sound attenuation are illustrated. Finally, by comparing measurements for thick and thin linings with predictions made using constrained and lubricated boundary conditions it is demonstrated that the manner in which lining materials are fitted into ducts can affect the sound attenuation.

1. INTRODUCTION

Resonators and porous lining materials are frequently used as economical solutions for reducing duct-borne noise that is an unwanted by-product of HVAC system operation [1]. While resonators can reduce noise considerably at only certain frequencies, porous lining materials can be used to reduce noise over a broad range of frequencies [2]. Thus, the use of resonators is limited to systems such as intake manifolds of automobiles where noise of only certain frequencies predominates. Porous duct linings are used more commonly since noise is generated over a wider range of frequencies in most cases.

Two categories of porous materials can be used to line the inside walls of ducts: fibrous media such as glass fiber and elastic porous materials such as foams. The two types of materials differ in the number of wave types that can propagate within them. It has been noted that an elastic porous material can convey two longitudinal wave types, while in fibrous media that can be modelled as either limp or rigid, only a single longitudinal wave is significant [3, 4]. More recent research revealed that elastic porous materials can simultaneously sustain an additional wave type, i.e., transverse waves, and that the interactions between the various types of propagating waves make the acoustical behavior of those materials more complicated and sensitive to boundary conditions than is the case for fibrous materials [5].

Sound propagation in a lined duct is generally studied by considering in-duct acoustical properties such as sound attenuation and phase speed. In 1939, Morse [6] proposed an

† Present address: Digital Appliance Research Laboratory, LG Electronics Inc., 327-23, Gasan-Dong, Keumchun-Ku, Seoul 153-023, South Korea.

0022-460X/01/020255 + 19 $35.00/0

analytical model for sound propagation within a lined duct. He derived a characteristic equation that governs sound propagation in the airway of lined ducts on the assumption that the liners were locally reacting. In that model, sound propagation within the liner material in the direction parallel to the duct was not modelled, but the effect of the liner on the sound field in the airway was accounted for by applying the normal incidence acoustic impedance at the interface between the liner and airway. Later, Scott [7] pointed out that Morse's locally reacting model was not valid under some circumstances, e.g., when the lining material is loosely packed or when the width of the airway is small compared with the wavelength. To overcome the shortcomings of Morse's model, he modelled liners as being bulk reacting and derived a characteristic equation that governed sound fields within both the liner and airway. In his model, only one longitudinal wave was assumed to propagate in the liner material, and the measured propagation constants and characteristic acoustic impedances of the lining materials were used to characterize the acoustical properties of the liner [8]. Sound attenuation predictions made using the Scott model were then compared with those made using Morse's model and with measurements. It was also shown that Scott's characteristic equation converges to Morse's characteristic equation when sound propagation in the airway is more dominant than that in the liner. Much later, Wassilief [9] extended, through extensive measurements, the validity of the duct attenuation model of Scott and of Kurze and Vér [10] to wider airway width and greater frequency range than those of previously published work.

The analytical models described above are, however, limited in their application to cases of lined ducts having regularly shaped cross-sections, i.e., rectangular or circular. Thus, there is a need to develop numerical models in order to analyze sound propagation in ducts of arbitrary cross-sectional shape. A finite element model of wave propagation along rectangular ducts lined with either extended or locally reacting porous materials was studied and its predictions were compared with extensive measurements [11]. Later, that numerical model was extended to other applications such as lined ducts with flexible walls, silencers of arbitrary cross-section and bar silencers [12–14]. In all cases, the porous lining materials that were considered were modelled as being extended or locally reacting and therefore could be considered to be effective fluids having complex wave numbers and densities, i.e., only one longitudinal wave was allowed to propagate within the liner.

A series of articles dealing with various fundamental aspects of poroelastic finite element formulations and the modelling of elastic porous materials for noise control use have been presented previously [15–18]: in all cases the poroelastic finite element formulation was based on the Biot theory for wave propagation in elastic porous media [19]. In the first of the four articles, the development of foam finite elements for homogeneous elastic porous materials in Cartesian co-ordinates and a method for coupling the foam finite elements with general acoustic elements are described [15]. By using the foam finite elements, the effect of edge constraints on the absorption coefficient of the finite-sized foam layer in a standing wave tube was demonstrated. In the second article, the foam finite element is extended to model the coupled acoustical–structural–foam system so as to be able to predict the sound transmission through finite, double-panel systems that are lined with plane, finite-depth foam layers [16]. In the third article, boundary conditions are described that allow the foam finite elements to be coupled to adjacent acoustical domains at arbitrarily angled interfaces [17]. By using the improved sound transmission prediction capability, it was shown that the transmission loss of a wedge-shaped foam treatment is significantly higher in some frequency bands than that of a plane treatment of the same volume. In the fourth article, an axisymmetric foam finite element is described that can easily and efficiently model axisymmetric sound propagation in circular structures having arbitrary, axially dependent radii, and that are lined or filled with elastic porous materials [18]. Predictions made using

the axisymmetric model were compared with measurements of sound transmission through cylindrical and conical foam plugs.

In the existing analytical and finite element work on the sound attenuation in lined ducts, only the cross-sections of the lined ducts have actually been modelled which nonetheless makes it possible to calculate the allowed axial wave numbers in the airway for every mode by assuming free wave propagation in the direction of the duct axis, i.e., an anechoic termination was assumed. It may thus be said that those models can be used to obtain the free responses of wave propagation in the lined ducts of infinite length. In those cases, the modelling is relatively simple and the decomposition of the fundamental and higher order mode components of the propagating waves is feasible. On the other hand, in the present study the whole lined duct of finite length including sound source and termination is modelled. It may thus be said that the forced responses of wave propagation in the lined ducts of finite length are considered. By using a realistic model of the type presented here, it is possible to account for the effect of termination impedance at low frequencies and that of mode contamination at high frequencies, effects which are usually observed in measurements.

In this paper, the sound attenuation and phase speed along circular ducts lined with elastic porous materials such as foams are studied by using the axisymmetric foam finite element model that was developed and validated in the previous work [18]. First, however, the axisymmetric foam finite element formulation and boundary conditions at the inner and outer surfaces of the lining materials are briefly described. Procedures for estimating the physical properties of polyurethane foams used in this study are presented. Predictions made using the finite element model are then compared with measurements of sound attenuation and phase speed along the lined ducts having various lining thicknesses for three different foams. Finally, the effect of constraining the outer circumferential surface of the foam liner on the sound attenuation is demonstrated.

2. FINITE ELEMENT MODEL OF CIRCULAR LINED DUCT

2.1. AXISYMMETRIC FINITE ELEMENT FORMULATIONS FOR LINER AND AIRWAY

Axisymmetrical problems such as lined ducts of circular cross-section may be modelled easily and efficiently by using axisymmetric finite elements. The axisymmetric poroelastic finite element model used in the present work was developed from the two wave equations governing sound propagation in elastic porous materials. The accuracy of that model has already been validated by comparing its predictions with predictions made using a three-dimensional finite element model and with measurement results for sound transmission through cylindrical and conical foam plugs placed in a hard-walled tube [18]. Since the detailed procedures are well described in reference [18], it will only be discussed very briefly here with a particular application to the circular lined duct.

It was shown in reference [18] that the axisymmetrical global foam finite element equations can be written in the form

$$[\mathbf{K}_f]\,\{\{\mathbf{u}_r\}\,\{\mathbf{u}_z\}\{\mathbf{U}_r\}\,\{\mathbf{U}_z\}\}^{\mathrm{T}} = \{\{\mathbf{F}^1\}\,\{\mathbf{F}^2\}\,\{\mathbf{F}^3\}\,\{\mathbf{F}^4\}\}^{\mathrm{T}} \tag{1}$$

where the vectors $\{\mathbf{u}_r\}$, $\{\mathbf{u}_z\}$, $\{\mathbf{U}_r\}$, and $\{\mathbf{U}_z\}$ are, respectively, the unknown displacement components of the solid and fluid phases of the foam (see Figure 1 for the co-ordinate systems), and $[\mathbf{K}_f]$ is the foam's global dynamic stiffness. In equation (2), the partitioned sub-matrices $\{\mathbf{F}^i\}$ are force vectors related to the normal and shear stresses acting on the

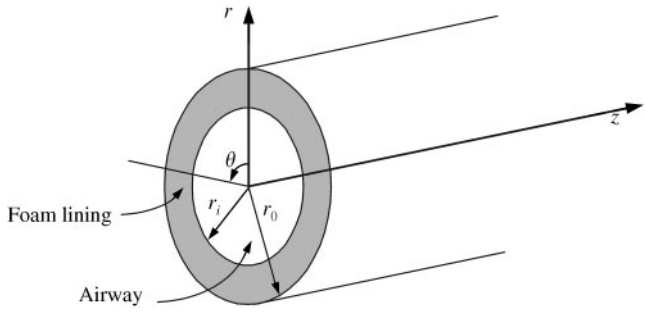

Figure 1. Co-ordinates for circular lined duct.

solid and fluid phases of the foam:

$$F_i^1 = \int_B r\phi_i(n_{fr}\sigma_r + n_{fz}\tau_{zr})\,\mathrm{d}B, \tag{2a}$$

$$F_i^2 = \int_B r\phi_i(n_{fr}\tau_{zr} + n_{fz}\sigma_z)\,\mathrm{d}B, \tag{2b}$$

$$F_i^3 = \int_B r\phi_i(n_{fr}s)\,\mathrm{d}B, \tag{2c}$$

$$F_i^4 = \int_B r\phi_i(n_{fz}s)\,\mathrm{d}B, \tag{2d}$$

where ϕ_i is the Lagrangian interpolation function, n_{fr} and n_{fz} are r and z components of the outward unit normal vector $\mathbf{n}_f$ on the boundary, σ_r, σ_z and τ_{zr} are the normal and shear stresses acting on the foam's solid phase, s is the normal stress acting on the foam's fluid phase, and B is the surface boundary.

For the acoustical domain, i.e., the airway of the duct shown in Figure 1, the axisymmetrical global acoustical finite element equations can be derived from the wave equation in a homogenous acoustic medium, and can be expressed as [18]

$$[\mathbf{K}_a]\,\{\mathbf{p}\}^{\mathrm{T}} = \{\mathbf{Q}\}^{\mathrm{T}}, \tag{3}$$

where

$$Q_i = -\,\mathrm{j}\omega\rho_0 2\pi \int_B r\phi_i(n_{ar}v_r + n_{az}v_z)\,\mathrm{d}B \tag{4}$$

Here $[\mathbf{K}_a]$ is the dynamic stiffness matrix of air, $\{\mathbf{p}\}$ is the vector of unknown nodal pressures, $\{\mathbf{Q}\}$ is the normal volume velocity flux vectors, v_r and v_z are, respectively, the radial and axial components of the acoustic particle velocity, $\mathbf{v}_a$, in the air, and n_{ar} and n_{az} are the corresponding components of the outward unit vector, $\mathbf{n}_a$, on the boundary.

2.2. BOUNDARY CONDITIONS AND COUPLING PROCEDURES

For the circular lined duct considered here, a foam system (i.e., the lining) can be coupled to a neighboring acoustical system (i.e., the airway) in the axisymmetric space by applying

appropriate boundary conditions that must be enforced at each node along the circumferential interface joining the two systems. At an open interface between the lining and airway, there are force and normal volume velocity compatibility conditions to be enforced in the radial and axial directions. Those conditions are

$$hp\mathbf{n}_a = s\mathbf{n}_f, \tag{5a}$$

$$(1-h)pn_a = r(\sigma_r n_{fr} + \tau_{zr} n_{fz})\mathbf{i} + r(\tau_{zr} n_{fr} + \sigma_z n_{fz})\mathbf{k}, \tag{5b}$$

$$\mathbf{v_a} = \mathrm{j}\omega(1-h)\mathbf{u} + \mathrm{j}\omega h\mathbf{U}, \tag{5c}$$

where h is the porosity, and $\mathbf{i}$ and $\mathbf{k}$ are, respectively, the unit vectors in the r and z directions.

Upon substituting boundary conditions (5a)–(5c) into equations (2a)–(2d) and equation (4), one can express all the flux vectors at the interface nodes in terms of nodal unknowns. It is then possible to place those terms in the proper position in the coupled dynamic stiffness matrix in a systematic way. The final axisymmetric acoustic–poroelastic system equations for the circular lined duct have the form

$$\begin{bmatrix} [\mathbf{K}_a] & [\mathbf{K}_{af1}] \\ [\mathbf{K}_{af2}] & [\mathbf{K}_f] \end{bmatrix} \{\{\mathbf{p}\}\,\{\mathbf{u}_r\}\,\{\mathbf{u}_z\}\,\{\mathbf{U}_r\}\,\{\mathbf{U}_z\}\}^{\mathrm{T}} = \{\{\mathbf{Q}\}\{\mathbf{F}^1\}\,\{\mathbf{F}^2\}\,\{\mathbf{F}^3\}\,\{\mathbf{F}^4\}\}^{\mathrm{T}}, \tag{6}$$

where $[\mathbf{K}_{af1}]$ and $[\mathbf{K}_{af2}]$ are the coupling matrices resulting from the coupling of the acoustical and poroelastic finite element equations. All the unknown vectors can now be found by applying other boundary conditions that are appropriate for the configurations to be considered, and solving the system equations simultaneously.

Two different sets of boundary conditions may apply when the foam lining is placed adjacent to the hard surface of the duct. When the foam lining can be placed easily into the tube (i.e., when the foam is not solidly attached to the hard surface, but simply rests against it), it is assumed that the foam is "lubricated". In this case, the tangential components of the foam's solid and fluid phases are unconstrained at the hard surface (i.e., both the solid and fluid phases may move freely along the hard surface), but the displacement components of both the foam's solid and fluid phases normal to the hard surface are set equal to zero, i.e.,

$$u_r = 0, \qquad U_r = 0 \tag{7a,b}$$

On the other hand, when the foam lining is tightly fitted into the duct (i.e., the foam is solidly connected to the hard surface), it is assumed that the foam is "constrained". That is, the tangential component of the solid phase motion must also be set equal to zero, as are the displacement components of both the foam's solid and fluid phases normal to the hard surface, i.e.,

$$u_r = 0, \qquad u_z = 0, \qquad U_r = 0 \tag{8a–c}$$

However, the tangential displacement component of the fluid phase within the foam is unconstrained at the hard surface, i.e., the fluid phase of the foam may slip at the boundary.

2.3. MODELLING DETAILS AND CALCULATIONS

Figure 2 shows a typical axisymmetric finite element model corresponding to an experimental set-up for measuring sound attenuation and phase speed in the circular lined

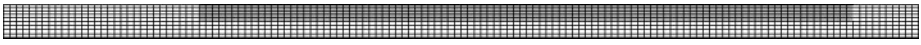

Figure 2. Typical finite element mesh for circular lined duct when open area fraction is 0·5.

TABLE 1

Measured and optimized macroscopic physical properties of foams

Parameter \ Foam type	Foam A	Foam B	Foam C
Flow resistivity (mks Rayls/m)	$1{\cdot}37 \times 10^4$	$3{\cdot}08 \times 10^4$	$4{\cdot}64 \times 10^4$
Tortuosity	3·58	4·28	6·13
Porosity	0·96	0·96	0·96
Bulk density (kg/m^3)	32	29	32
Bulk Young's modulus (Pa)	$3{\cdot}04 \times 10^4$	$2{\cdot}52 \times 10^4$	$8{\cdot}58 \times 10^4$
Loss factor	0·3	0·3	0·3
The Poisson ratio	0·4	0·4	0·4

duct, for which measurement procedures will be described in section 3.4. The gray elements represent the foam lining and the white elements represent the airway and the airspaces upstream and downstream of the lined section. The lower edge of the model represents the axis of symmetry while the upper edge represents the duct circumference. All of the elements in the axisymmetric model were four-node, linear quadrilateral elements. In the case of the thickest lining as shown in Figure 2, the model comprised 500 foam elements and 900 acoustical elements for a total of 1400 elements having 1551 nodes.

Unit amplitude axial velocities were prescribed at the nodes of the left-hand side of the upstream section in order to generate a plane wave travelling in the positive axial direction. An anechoic termination of impedance $\rho_0 c$ was imposed at the nodes of the right-hand end of the downstream airspace. At its circumferential edges, the foam lining was assumed to be either fully constrained (i.e., $u_r = 0$, $u_z = 0$ and $U_r = 0$ at $r = r_o$) or lubricated (i.e., $u_r = 0$ and $U_r = 0$ at $r = r_o$) to illustrate the effect of boundary conditions.

By using the complex pressures at the nodes of $r = 0$ in the airway that were obtained from equation (6), the sound attenuation and phase speed were calculated in the same way as done for their measurements that will be described in section 3.4.

The parameters for the foam samples used in the present calculations are listed in Table 1. These values were obtained by the procedures to be described in section 4.

3. MEASUREMENTS OF PHYSICAL AND ACOUSTICAL PROPERTIES

3.1. SAMPLE PREPARATION

Three types of polyurethane foam buns were manufactured, namely foams A–C. Foams A and C were ester based and foam B was ether based. First, four circular cylinders having diameters of 10 cm and lengths of 1 m were carefully cut from each bun. Foam lining samples were then fabricated by cutting the cylindrical foam samples into a hollow cylindrical shape for measurements of sound attenuation and phase speed. The inner diameters of the foam linings were specified in terms of the "open area fraction", which was defined as the ratio of the inner radius to the outer radius of the lining, i.e., r_i/r_o in Figure 1 [20]. Four different open area fractions, 0·5, 0·6, 0·7 and 0·8, were considered here for sound attenuation and phase speed.

It is common experience that most porous materials are spatially inhomogeneous, i.e., their macroscopic properties vary randomly throughout the material [21]. Nonetheless, none of the currently popular porous material theories explicitly accounts for the spatial inhomogeneity of macroscopic properties. Thus, insofar as this effect is acknowledged, the "properties" of a porous material are usually estimated from measurements made using a number of individual samples. In the present study, 10 samples for each of three types of polyurethane foams were used to estimate the physical properties. From the same bun from which the foam lining samples were cut, 10 circular cylinders having a diameter of 10 cm and a thickness of 5 cm were also cut for measurements of the flow resistivity and absorption coefficient.

3.2. FLOW RESISTIVITY

The experimental apparatus for measuring the airflow resistivity of polyurethane foams in the present work was based on the set-up published by ASTM [22]. The basic schematics and the actual set-up are shown in Figure 3. A plastic transparent tube 20 cm long, having a diameter of 10 cm, was used as the sample holder. A 5 cm thick foam sample with a diameter of 10 cm was placed against a removable screen held in position 5 cm above the mounting plate. The downstream side of the sample holder was connected to an ejector that induced low pressure from a high-pressure airflow. By blowing the high-pressure airflow into the ejector, a low and steady airflow through the foam sample could be obtained. The rate of airflow could be controlled by using a regulator that controlled the rate at which the high-pressure airflow was supplied to the ejector. A Setra 264 pressure transducer having measurement ranges of either 0–0·1 or 0–1·0 in H_2O was attached to the sample holder to measure the pressure difference across the sample. A DWYER flowmeter having a range of 0–5000 ml/min was used to measure the volume flow rate of air through the sample. By adjusting the airflow rate, data sets for various volume flow rates of air and the corresponding pressure differentials across the sample could be obtained. The ratio of pressure differential to volume flow rate was given by the linear coefficient of a first order least-squares fit. The flow resistivity r_0 was then obtained from the expression $r_0 = \Delta PA/\forall t$ by relating the ratio of pressure difference to volume flow rate to the flow resistivity. Here, ΔP is the pressure differential across the sample, $\forall$ is the volume flow rate of air, A is the cross-sectional area of sample and t is the sample thickness.

3.3 SOUND ABSORPTION COEFFICIENT

The normal incidence absorption coefficient was measured by using a Brüel and Kjær two-microphone impedance measurement tube (Type 4206) based on the ASTM E 1050

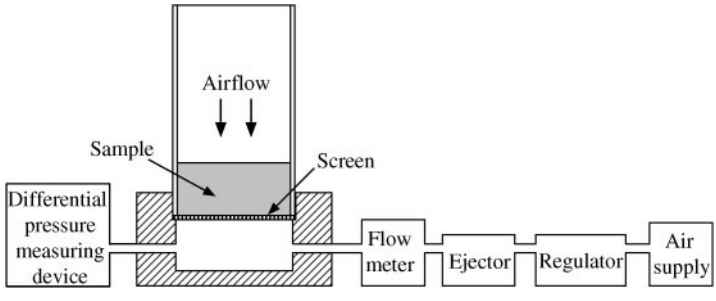

Figure 3. Set-up for measurement of flow resistivity.

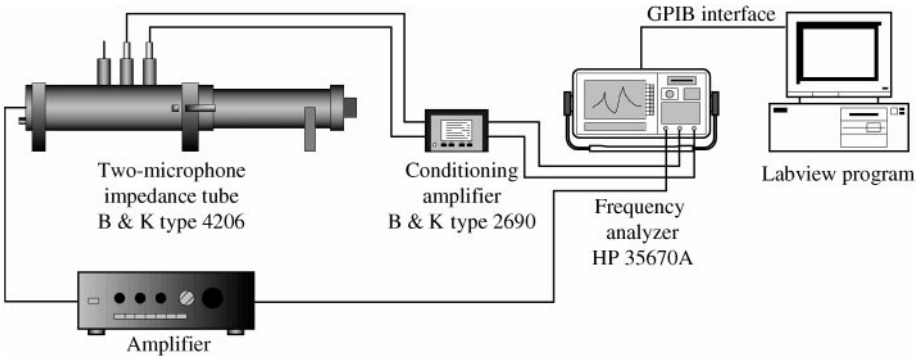

Figure 4. Set-up for measurement of absorption coefficient using a tube and two microphones.

standard [23]. The schematic representation of the experimental apparatus is shown in Figure 4. The test apparatus consisted of a tube of constant cross-section with a loudspeaker at one end and provision for holding a sample at the other end. The same foam sample that was used for the flow resistivity measurements was carefully placed in the sample holder. A broadband signal of 50 Hz up to 1600 Hz was generated by an HP 35670A dynamic signal analyzer, passed through a power amplifier and delivered to the loudspeaker to generate a plane standing wave field in the tube. The transfer function between the two microphones flush mounted to the interior surface of the tube was measured by using the signal analyzer. The measured data were automatically transferred and stored in a PC by using GPIB interface and LABVIEW software. The absorption coefficient could then be estimated from the transfer function and the positions of the microphones with respect to the sample.

3.4. SOUND ATTENUATION AND PHASE SPEED

A modified Brüel and Kjær two-microphone impedance measurement tube (Type 4206) was used to make measurements of sound attenuation and phase speed in the airway of the circular foam-lined duct. The modifications to the standard tube were as follows. First, extension tubes having the same inner diameter (10 cm) as the standard impedance tube, two of 50 cm length and one of 60 cm length were machined to increase the total length of the measurement set-up. The extension tubes of stainless steel were coated to decrease surface roughness and to protect them from rust. The tubes were connected by large plastic nuts that were carefully fabricated to minimize the pressure leakage in the connections. A test section comprising two 50 cm long sections was then positioned between the Brüel and Kjær large measurement tube (Part UA 1117) and a 60 cm long anechoic termination. The final configuration is illustrated schematically in Figure 5.

A lining sample was carefully inserted into the test section: thick linings appeared to fit tightly while thin linings seemed to fit smoothly: the acoustical effect of this difference will be shown by demonstrating the effect of boundary conditions in section 5. The anechoic termination was fabricated from loosely packed crumbled foams of several types: this material was held in place by thin foam plugs. It was intended that the termination have an absorption coefficient greater than 0·95 at all frequencies higher than 100 Hz. The performance of the actual termination is shown in Figure 6. It can be seen that the design goal was satisfied, and that the absorption coefficient was in fact greater than 0·97 at all frequencies greater than 300 Hz.

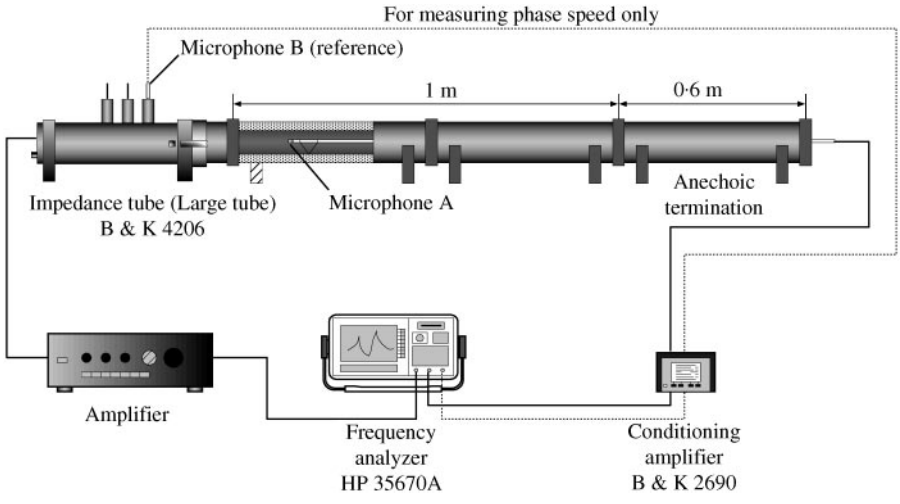

Figure 5. Set-up for measurements of sound attenuation and phase speed.

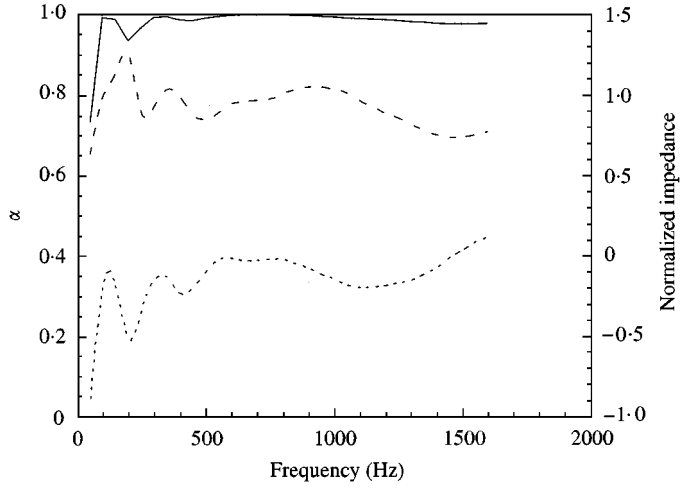

Figure 6. Measured absorption coefficient and impedance of anechoic termination: ——, absorption coefficient; - - - -, impedance (real part); —, impedance (imaginary part).

Pure tone signals at the one-third octave band center frequencies in the range 100 Hz–10 kHz were generated by using an HP35670A dynamic signal analyzer and were then passed through a power amplifier before being delivered to the loudspeaker. The sound field at the center of the airway of the lined duct was measured at nine different locations by using a 1/4″ microphone (Brüel and Kjær Type 4187) that was guided by a probe tube and connected to the signal analyzer. The measurement locations were spaced 10 cm apart, starting from a position 10 cm from the inlet of the test section. The measured sound pressure level was found to decay nearly linearly with distance from the duct inlet, although a standing wave pattern was evident at frequencies below 150 Hz. The sound attenuation per unit length was then calculated from the linear coefficient of a first order leasts squares fit of the measured sound pressure level versus position data.

Measurements for phase speed in the airway were divided into low- and high-frequency ranges to reduce equipment dynamic range requirements. In the low-frequency test, a random noise input signal to the loudspeaker was bandlimited to span 100 Hz–1.6 kHz, while in the high-frequency test pure tone signals at the one-third octave band center frequencies, spanning 2–10 kHz, were used. The transfer function between a reference signal measured directly in front of the loudspeaker and the microphone output at each of the six measurement positions was measured by using the signal analyzer. The measurement locations started from a position 15 cm away from the inlet of the test section. The distance between the adjacent measurement points was 5 cm for the low-frequency test and 1 cm for the high-frequency test. The phase speed could then be given by averaging the results that were obtained using the following relationship:

$$c = f\lambda = f\frac{2\pi d}{\theta_{i+1} - \theta_i} \quad (i = 1, 3, 5),$$

where θ_i is the phase angle of the transfer function at the ith measurement position and d is the distance between the adjacent measurements.

4. ESTIMATION OF FOAM PARAMETERS

Elastic porous material theories are generally formulated in terms of seven or more macroscopically measurable physical properties of the frame (i.e., the solid phase) and the fluid [5, 24]. Those properties are the flow resistivity, the tortuosity, the porosity, the bulk density, the *in vacuo* bulk Young's modulus, the associated loss factor and the Poisson's ratio. The first three physical parameters together constitute the material's fluid-acoustical properties and the last four properties comprise the elastic properties of the materials. Most of the properties are, in principle, measurable although some of them are more often determined by matching theoretical and experimental results. As noted in previous studies [5, 21], some of them (e.g., the flow resistivity, the tortuosity and the bulk Young's modulus) can significantly affect the acoustical behaviors of foams while others (e.g., the porosity) have little effect and tend to vary over narrow ranges. In the present study, the flow resistivity and the bulk density were measured, and the porosity, the loss factor and the Poisson ratio were assumed to have typical values for the properties of polyurethane foams. The tortuosity and the bulk Young's modulus were then estimated through an optimization process that involved minimizing the difference between the predicted and measured normal incidence sound absorption coefficient of a finite depth of foam sample placed in a hard backing. The theoretical predictions were made by using an analytical model [5] that itself was also based on the Biot theory. The normal incidence absorption coefficient was measured using the two-microphone impedance tube as described in section 3.3. The optimization was performed using the results in the frequency range 50 Hz–1·6 kHz since the samples were available only for the large measurement tube having a diameter of 10 cm. The physical properties of the three types of foam samples are listed in Table 1. The listed values for the flow resistivity and the bulk density are averaged values from measurements for the 10 samples. The listed values for the tortuosity and the bulk Young's modulus are averaged values from the parameters that were optimized for each of the 10 sets of measured data. As may be seen from Table 1, foam C had much larger nominal values of flow resistivity, tortuosity and bulk Young's modulus than foam A, although both the foam samples had the same bulk density. It may thus be said that foam C had a stiffer frame and a more complicated interstitial structure than foam A. Foam B had values that were intermediate between foams A and C. In Figure 7, the measured absorption coefficients are

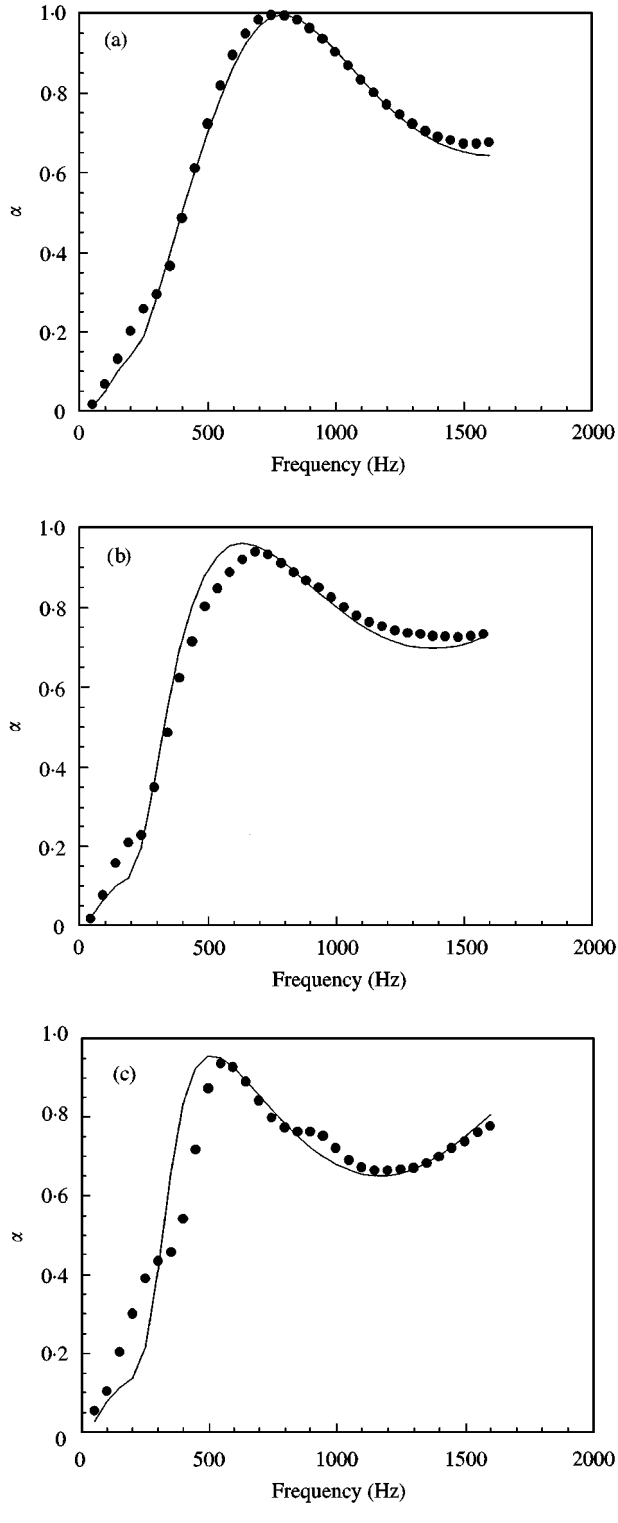

Figure 7. Comparison of measured and predicted absorption coefficients (a) foam A, (b) foam B, (c) foam C: ●, measured; ——, predicted using optimized properties.

compared with predictions made using the properties listed in Table 1. It may be seen that the predictions are generally in very good agreement with the measurements, although there are some differences at low frequencies below 600 Hz. Those differences presumably result from constraint of the circumferential surface of the foam samples since the foam C samples were placed in the sample holder relatively tightly due to their higher stiffness [18].

5. RESULTS AND DISCUSSION

Four configurations having different open area fractions were considered for each of the three types of foams A, B and C. Figures 8–10 show the measured results and finite element predictions for the sound attenuation and phase speed in the airway of the foam-lined circular ducts. Some discrepancies between measurements and predictions are evident at frequencies below 400 Hz and at high frequencies above 4 kHz, but the general agreement is reasonable. Considering that the wavelength at 400 kHz is 0·8575 m in free-field conditions, the test section used in the present work was not long enough to measure sound attenuation

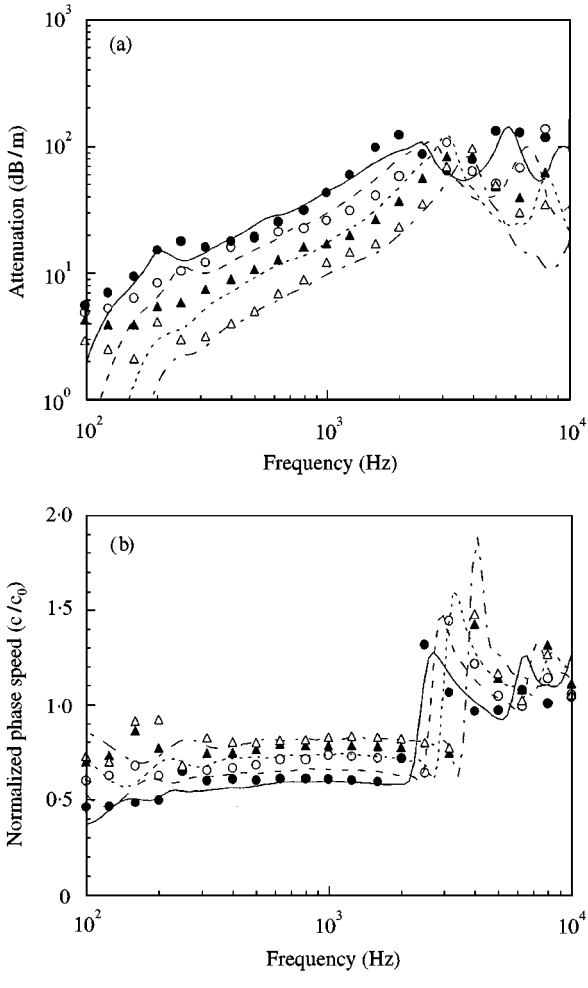

Figure 8. Wave propagation properties for foam A. (a) sound attenuation, (b) normalized phase speed: ——, – – – –, - - - - -, –·–·–, FEM results for open area fractions 0·5, 0·6, 0·7 and 0·8 respectively; ●, ○, ▲, △, measurements for open area fractions 0·5, 0·6, 0·7 and 0·8 respectively.

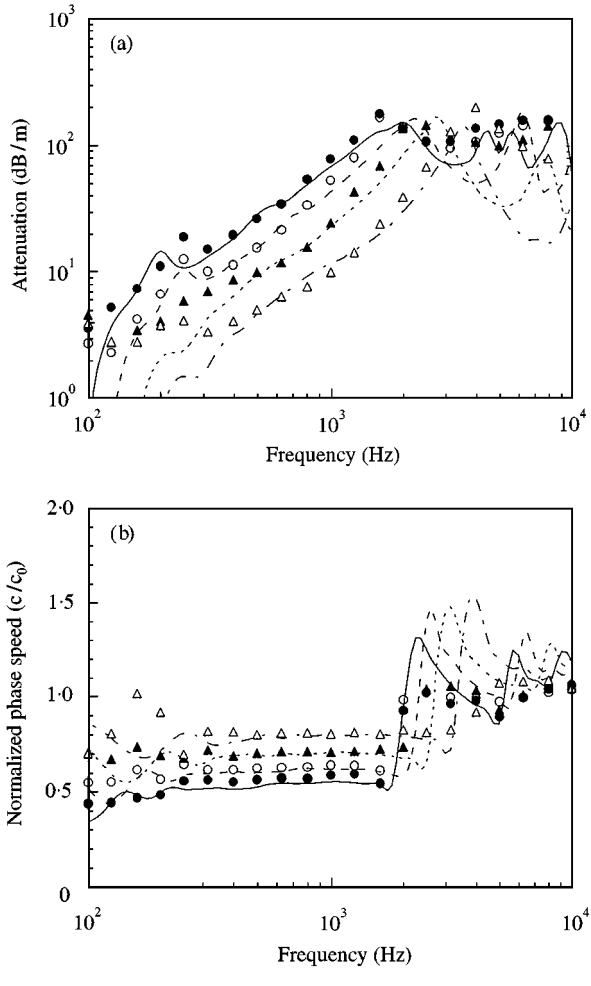

Figure 9. Wave propagation properties for foam B. (a) sound attenuation, (b) normalized phase speed: ——, – – – –, - - - - -, – · – · –, FEM results for open area fractions 0·5, 0·6, 0·7 and 0·8 respectively; ●, ○, ▲, △, measurements for open area fractions 0·5, 0·6, 0·7 and 0·8 respectively.

accurately at frequencies below 400 kHz. Moreover, owing to reflection from the "anechoic" termination, standing wave patterns appear in the measured sound pressure levels at low frequencies. In addition, when the sound attenuation rate was too high, there were some disagreements between the measurements and predictions at high frequencies. Note also that it was assumed in the predictions that the foam linings were fully constrained for the cases of open area fractions of 0·5 and 0·6 while the foam linings were assumed to be lubricated for the cases of open area fractions of 0·7 and 0·8. The reason for applying different boundary conditions and the corresponding acoustical effects will be discussed later in this section. It may be seen from Figures 8 to 10 that the sound attenuation increases and the phase speed decreases as the thickness of the lining increases. As may also be seen from Figures 8 to 10, the phase speed remains almost constant until the cut-on of the first symmetric mode (between 1 and 2 kHz). The phase speed rapidly increases at the cut-on frequency, above which the phase speed decreases with frequency until the cut-on of the second symmetric mode (between 4 and 6 kHz). On the other hand, the sound attenuation

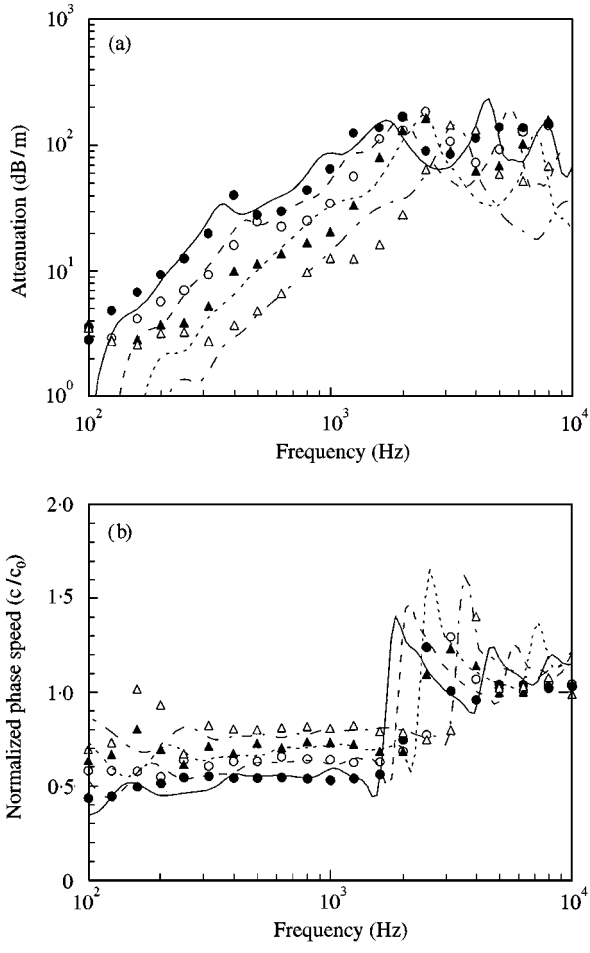

Figure 10. Wave propagation properties for foam C. (a) sound attenuation, (b) normalized phase speed: ——, – – – –, - - - - -, –·–·–, FEM results for open area fractions 0·5, 0·6, 0·7 and 0·8 respectively; ●, ○, ▲, △, measurements for open area fractions 0·5, 0·6, 0·7 and 0·8 respectively.

gradually increases with frequency until the cut-on of the first symmetric mode decreases while that mode dominates, and increases again until the cut-on of the second symmetric mode.

A comparison of the finite element predictions for an open area fraction of 0·6 for foam types is shown in Figure 11. While foam C gives the highest sound attenuation and rate of increase of attenuation above 300 kHz, there are only slight differences in the phase speeds below the higher order mode cut-on frequencies. It is interesting to note that increases in the flow resistivity and the tortuosity cause the cut-on frequencies to be decreased.

In Figure 12, the finite element predictions are compared with Morse's analytical solutions [6] and with measurements for the cases of open area fractions of 0·5 and 0·8. Morse's analytical solution procedure is also described briefly in Appendix A. There are large differences between Morse's predictions and the finite element results in the former case (i.e., when the linings are thick). However, Morse's predictions agree reasonably well with measurements and finite element results in the latter case (i.e., when the linings are thin), although Morse's predictions are not accurate in the vicinity of modal cut-on

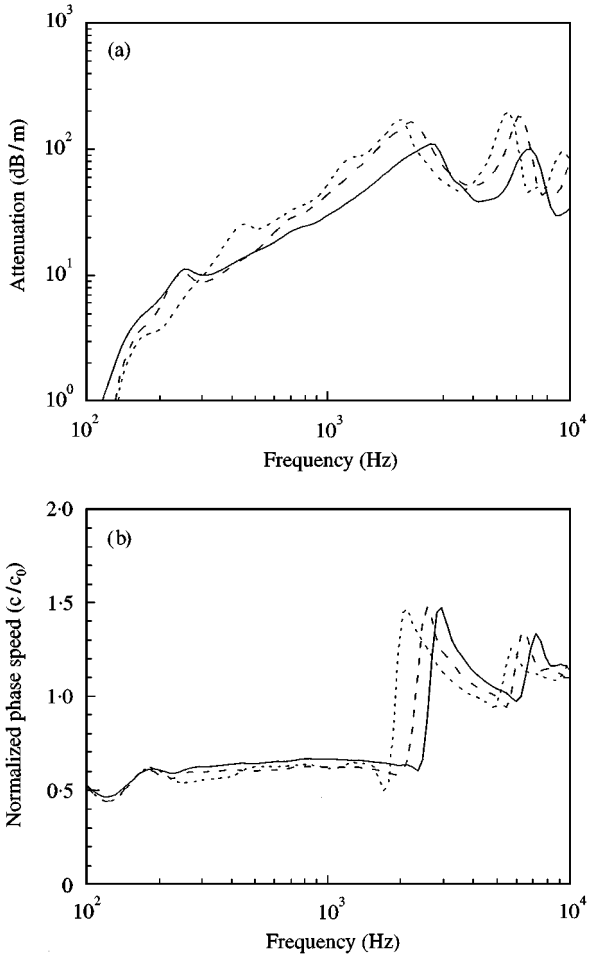

Figure 11. Effect of foam's properties when open area fraction is 0·6 (a) sound attenuation, (b) phase speed: ——, foam A; – – – –, foam B; - - - - -, foam C.

frequencies. When the lining thickness is small compared to the radius of the airway, the sound field at the center of the airway is little affected by the lining materials because the interaction between the sound fields within the lining and within the airway is weak. It may thus be concluded that Morse's solution can be used as an approximation of the present extended model below modal cut-on frequencies in which cases the sound propagation in the airway is more dominant than that in the lining (typically when the lining is thin).

During the measurements it was found that the sound attenuation was affected by the manner in which the samples fit into the test section of the duct. The thick linings having open area fractions of 0·5 and 0·6 fit tightly against the duct wall while the thin linings having open area fractions of 0·7 and 0·8 fit smoothly. To illustrate the effect of boundary conditions on the sound attenuation, measurements were compared with predictions when two different sets of boundary conditions (i.e., constrained and lubricated boundary conditions) were imposed at the outer circumferential surface of the linings for the two extreme cases of 0·5 and 0·8. As may be seen from Figure 13, constraining the circumferential edge of the lining apparently increases the sound attenuation at a low-frequency region, an effect that is visible in both the measured and predicted results.

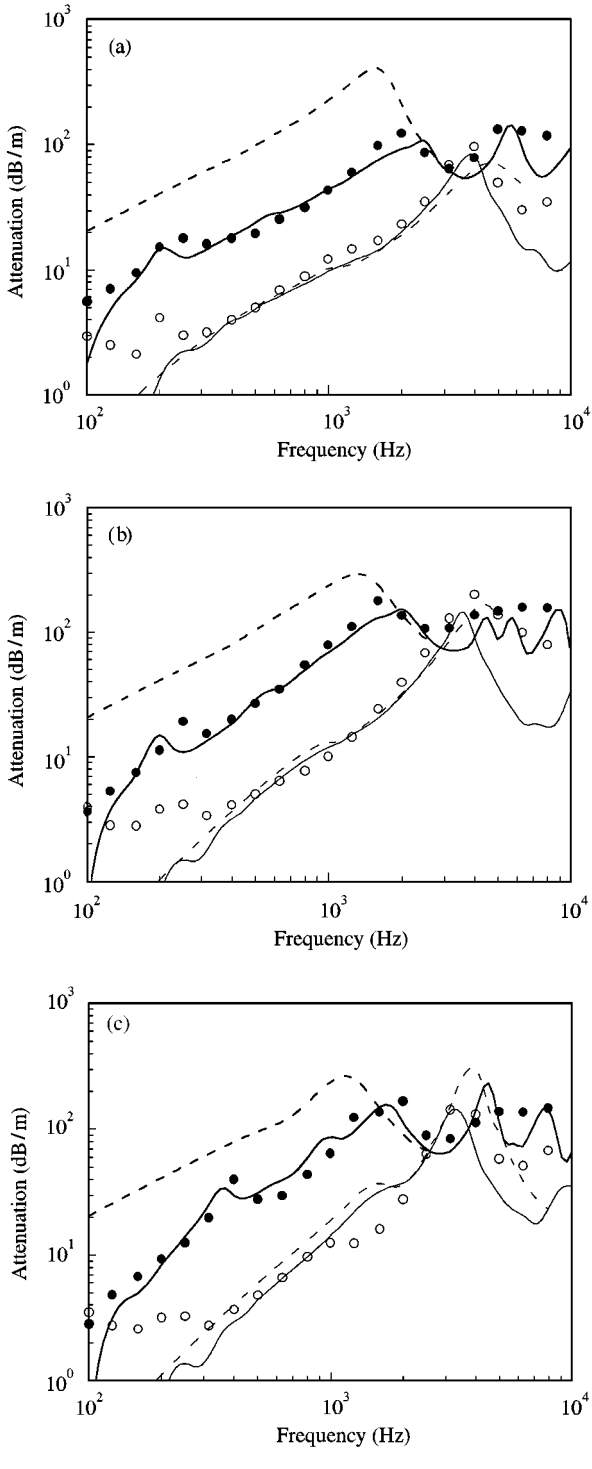

Figure 12. Comparison of Morse's solutions, FEM predictions and measurements (a) foam A, (b) foam B, (c) foam C: —, —, FEM results for open area fractions 0·5 and 0·8 respectively; - - -, – – –, Morse's solution for open area fractions 0·5 and 0·8 respectively; ●, ○, measurements for open area fractions 0·5 and 0·8 respectively.

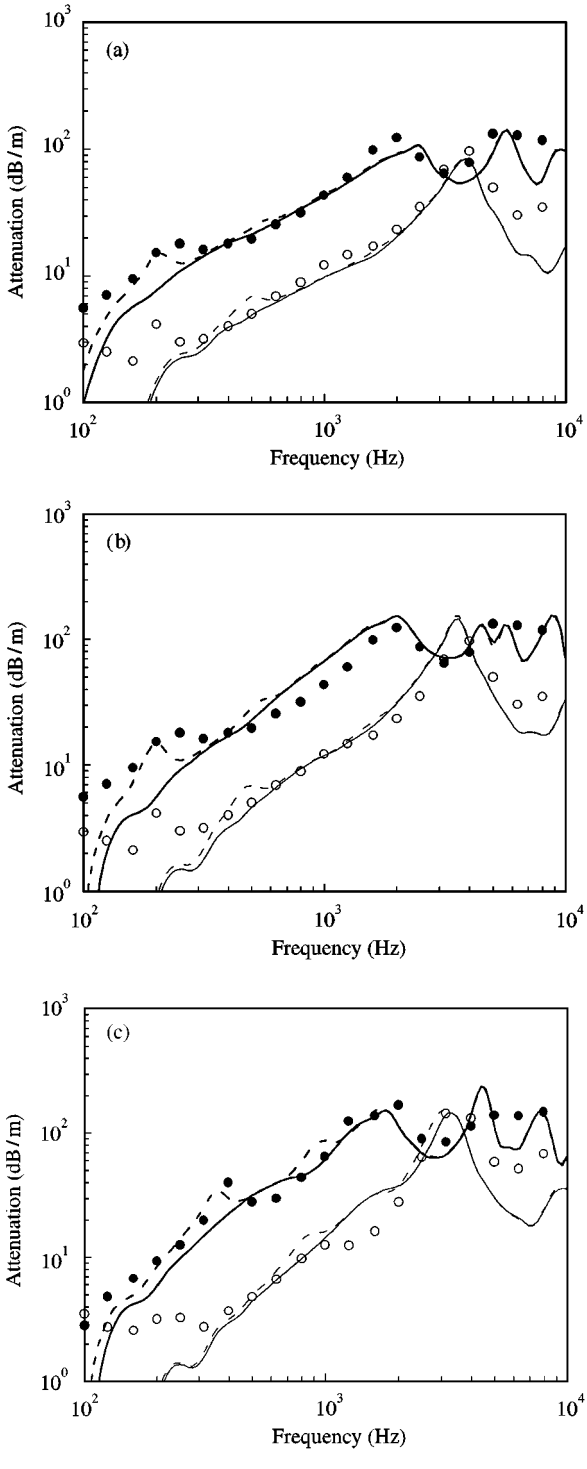

Figure 13. Effect of boundary conditions on sound attenuation (a) foam A, (b) foam B, (c) foam C: —, —, FEM results (constrained) for open area fractions 0·5 and 0·8 respectively; - - -, – – –, FEM results (lubricated) for open area fractions 0·5 and 0·8 respectively; ●, ○, measurements for open area fractions 0·5 and 0·8 respectively.

The increase in sound attenuation was found to be more significant when the linings were made thicker. Hence, it is appropriate to apply different boundary conditions depending on the degree of constraint of the solid phase at the outer surface of the lining. Recall that in the calculation presented above, the constrained boundary conditions were imposed for the cases of open area fractions 0·5 and 0·6, and the lubricated boundary conditions were used in the cases of open area fractions 0·7 and 0·8.

6. CONCLUSIONS

An axisymmetric foam finite element formulation has been used to predict the sound attenuation and phase speed in circular ducts lined with polyurethane foams. It has been demonstrated that a set of macroscopic physical properties obtained using an optimization procedure can be used to reproduce, with reasonable accuracy, measured sound attenuation and phase speed in foam-lined ducts having various open area fractions. It has also been shown that difficulties in measurements can occur at very low frequencies and beyond the cut-on frequencies of higher order modes. It has been shown that the sound attenuation increases at high frequencies but decreases at low frequencies as the flow resistivity and tortuosity of the linings become higher. Finally, it has been found that constraint of the circumferential surfaces of the linings increases the sound attenuation at low frequencies.

ACKNOWLEDGMENTS

The authors would like to thank Dr J. Stuart Bolton and the referees for their valuable suggestions, comments and constructive criticism. The authors would also like to thank Hongki Chung at Hanil Aero Machinery Co. Ltd. for the assistance in the design and fabrication of the experimental setup.

REFERENCES

1. I. L. VÉR 1978 *American Society of Heating, Refrigerating and Air Conditioning Engineers Transactions* **84**, 122–149. A review of the attenuation of sound in straight lined and unlined ductwork of rectangular cross section.
2. L. E. KINSLER, A. R. FREY, A. B. COPPENS and J. V. SANDERS 1982 *Fundamentals of Acoustics*. New York: Wiley, third edition.
3. C. ZWIKKER and C. W. KOSTEN 1949 *Sound Absorbing Materials*. New York: Elsevier.
4. L. L. BERANEK 1947 *Journal of the Acoustical Society of America* **19**, 556–568. Acoustical properties of homogeneous, isotropic rigid tiles and flexible blankets.
5. J. S. BOLTON, N.-M. SHIAU and Y. J. KANG 1996 *Journal of Sound and Vibration* **191**, 317–347. Sound transmission through multi-panel structures lined with elastic porous materials.
6. P. M. MORSE 1939 *Journal of the Acoustical Society of America* **11**, 205–210. The transmission of sound inside pipes.
7. R. A. SCOTT 1946 *Proceedings of the Physical Society* **58**, 358–368. The propagation of sound between walls of porous material.
8. R. A. SCOTT 1946 *Proceedings of the Physical Society* **58**, 165–183. The absorption of sound in a homogeneous porous material.
9. C. WASSILIEFF 1986 *Journal of Sound and Vibration* **114**, 239–251. Experimental verification of duct attenuation models with bulk reacting linings.
10. U. J. KURZE and I. L. VÉR 1972 *Journal of Sound and Vibration* **24**, 177–187. Sound attenuation in ducts lined with non-isotropic material.
11. R. J. ASTLEY and A. CUMMINGS 1987 *Journal of Sound and Vibration* **116**, 239–263. A finite element scheme for attenuation in ducts lined with porous material: comparison with experiment.

12. R. J. ASTLEY, A. CUMMINGS and N. SORMAZ 1991 *Journal of Sound and Vibration* **150**, 119–138. A finite element scheme for acoustic propagation in flexible-walled ducts with bulk-reacting liners, and comparison with experiment.
13. A. CUMMINGS 1995 *Journal of Sound and Vibration* **187**, 23–37. A segmented Rayleigh–Ritz method for predicting sound transmission in a dissipative exhaust silencer of arbitrary cross-section.
14. A. CUMMINGS and R. J. ASTLEY 1996 *Journal of Sound and Vibration* **196**, 351–369. Finite element computation in bar-silencers and comparison with measured data.
15. Y. J. KANG and J. S. BOLTON 1995 *Journal of the Acoustical Society of America* **98**, 635–643. Finite element modeling of isotropic elastic porous materials coupled with acoustical finite elements.
16. Y. J. KANG and J. S. BOLTON 1996 *Journal of the Acoustical Society of America* **99**, 2755–2765. A finite element model for sound transmission through foam-lined double panel structures.
17. Y. J. KANG and J. S. BOLTON 1997 *Journal of the Acoustical Society of America* **102**, 3319–3332. Sound transmission through elastic porous wedges and foam layers having spatially graded properties.
18. Y. J. KANG, B. K. GARDNER and J. S. BOLTON 1999 *Journal of the Acoustical Society of America* **106**, 565–574. An axisymmetric poroelastic finite element formulation.
19. M. A. BIOT 1956 *Journal of the Acoustical Society of America* **28**, 168–191. Theory of propagation of elastic waves in a fluid-saturated porous solid. I. Low-frequency range. II. Higher frequency range.
20. K. U. INGARD 1994 *Notes on Sound Absorption Technology*, 6–8. New York: Noise Control Foundation.
21. W. TSOI 1992 *MS thesis, School of Mechanical Engineering, Purdue University*. Acoustical modeling of polyimide foams.
22. *ASTM Standards* C 552-87. Standard test methods for airflow resistance of acoustical materials.
23. *ASTM Standards* E 1050-90. Impedance and absorption of acoustical materials using a tube, two microphones, and a digital frequency analysis system.
24. K. ATTENBOROUGH 1982 *Physics Reports* **82**, 179–227. Acoustical characteristics of porous materials.

APPENDIX A: MORSE'S LOCALLY REACTING MODEL

By applying the surface normal impedance at the interface between the lining and airway, one can derive a characteristic equation for wave propagation within the circular lined duct as follows, i.e.,

$$\frac{\mathbf{J}_1(bk_r)}{\mathbf{J}_0(bk_r)} = -i\frac{k}{k_r}\frac{1}{z'}$$

$$k_z = \sqrt{k^2 - k_r^2}.$$

Here, b is the radius of duct airway, z' is the surface normal impedance, k_r is the complex wave number in *the r* direction, and k_z is the complex wave number in the z direction. Sound attenuation can then be calculated as $8{\cdot}6858\ \mathrm{Im}(k_z)$ (dB/m).